

Designing All-Polymer Nanostructured Solid Electrolytes: Advances and Prospects

Emmanouil Glynnos,* Christos Pantazidis, and Georgios Sakellariou*



Cite This: *ACS Omega* 2020, 5, 2531–2540



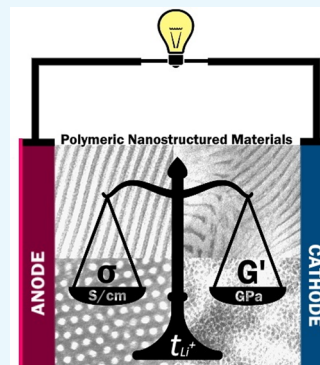
Read Online

ACCESS |

Metrics & More

Article Recommendations

ABSTRACT: Multi-phase nanostructured polymer electrolytes, where the one phase conducts ions while the other imparts the desired mechanical properties, are currently the most promising candidates for solid-state electrolytes in high-density lithium metal batteries. In contrast to homogeneous polymer electrolytes, where ion transport is coupled with polymer segmental dynamics and any attempt to improve conductivity via faster polymer motions results in a decrease in stiffness, nanostructured materials efficiently decouple these two antagonistic parameters. Nevertheless, for reasons discussed herein the synthesis of a polymer electrolyte that simultaneously has a shear modulus of $G' \approx \text{GPa}$ and an ion conductivity of $\sigma > 10^{-4} \text{ S/cm}$ (in the case dual ion conductor) or of $\sigma > 10^{-5} \text{ S/cm}$ (in the case of single-ion conductor) remains a challenge. This review focuses on recent designing strategies for the synthesis of all-polymer nanostructured electrolytes, and protocols for introducing a single-ion character in such materials.



1. INTRODUCTION

Climate change, pollution, and declining fossil resources are overwhelming challenges to humankind. Gaseous emissions from burning fossil fuels and biomass are not only polluting the air over large modern cities but are also creating alarming climate changes. Furthermore, it is universally recognized that national vulnerabilities and social instabilities can be created by a foreign dependence on fossil fuels. These concerns lead to national initiatives to reconsider the use of alternative energy sources such as solar radiation, wind, and waves. However, the intermittence of these resources, since they are variable in time and diffuse in space, requires high-efficiency energy storage systems. If a future economy based on renewable energy sources is to become reality, we will need to develop compact, safe, lightweight, high-capacity rechargeable batteries with longer life/cycles.^{1,2} At present, the definitive route to increase the energy density of the currently used, commercial available, Li ion battery (LIB) is the incorporation of metallic lithium as the anode material.^{3,4} For a given cathode material, metallic lithium maximizes the cell voltage and has a specific anode capacity nearly ten times larger than the currently used lithium-intercalating graphite anodes and gives the maximum possible energy density of any anode material. Lithium metal is the lightest (atomic mass of 7 g mol^{-1}), one of the most reducing of metals (electrochemical potential of -3.04 V , measured against the standard hydrogen electrode) and therefore holds the highest possible energy density for a negative electrode.

Today, LIBs represent a multibillion-dollar industry as the power supply of cellular phones, tablets, laptops, and other hand-held electronic devices. The currently used LIBs are

composed of a liquid electrolyte, which is a mixture of a lithium salt dissolved in an organic solvent, sandwiched between two lithium-intercalating electrodes. Despite their high ionic conductivity, liquid electrolytes are incompatible with lithium metal with many safety issues. Presently the most difficult challenge to the development of lithium metal batteries (LMBs) stems from the uneven dendritic lithium electrodeposition on the negative electrode.^{3,4} Once nucleated, the growing dendrites have at least two harmful consequences on battery operation. First, the high surface area structures continuously react with the electrolyte solvent to form solid electrolyte interface, consuming the electrolyte and eventually causing premature battery failure. Second, dendrites eventually short circuit the battery cell, as they create an electron-conductive connection between the two electrodes. When a flammable electrolyte is used, the dendrite-induced short is both a potential fire and explosion hazard, leading to catastrophic battery failure.⁵

After the theoretical prediction by Monroe and Newman⁶ that a mechanically robust electrolyte with a shear modulus, G' , of order of GPa would mechanically suppress/block macroscopic dendrite formation and growth, significant research efforts have focused on the development of solid-state electrolytes, capable of eliminating dendrite formation

Received: December 2, 2019

Accepted: January 30, 2020

Published: February 10, 2020

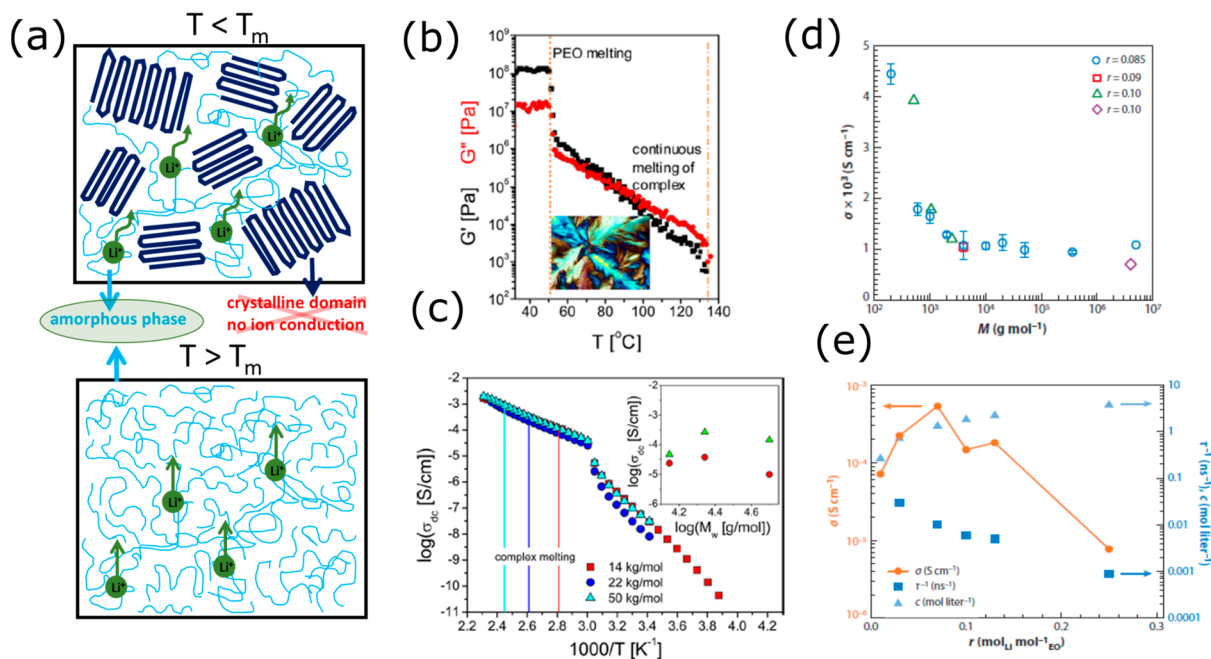


Figure 1. (a) Schematic depicting Li^+ transport in (top) crystallized PEO electrolytes, i.e., at $T < T_m$, and (bottom) in fully amorphous PEO electrolytes, i.e., at $T > T_m$. (b) Temperature dependence of the storage (G' , black symbols) and loss (G'' , red spheres) moduli of linear PEO ($M_w = 22 \text{ kg/mol}$) doped with LiCF_3SO_3 at $[\text{EO}]/[\text{Li}] = 12$. (c) Ion conductivity of homopolymer PEO doped with LiCF_3SO_3 at $[\text{EO}]/[\text{Li}] = 8$ for different molecular weights of PEO; the inset is the ionic conductivities for $[\text{EO}]/[\text{Li}] = 8$ (up triangles) and $[\text{EO}]/[\text{Li}] = 4$ (red spheres) as a function of PEO molecular weight at the same temperature above melting (Reprinted from the work of Zardalidis et al.¹¹ Copyright 2013. American Chemical Society). (d) Ion conductivity as a function of PEO molecular weight for different LiTFSI salt concentrations, $r = [\text{Li}]/[\text{EO}]$. (e) Ion conductivity (orange cycles, left axis), polymer segmental dynamics (dark blue squares, right axis), and salt concentration (light blue triangles, right axes) vs salt molar ration (Reprinted from the work of Hallinan et al.¹⁰ Copyright 2013. Annual Review).

while exhibiting high ionic conductivity at room temperature. Solid-state electrolytes fall mainly into two categories: inorganic ceramic electrolytes and solid polymer electrolytes. Despite the fact that inorganic ceramics exhibit satisfactory ionic conductivity and mechanical properties that range from tens to hundreds of GPa, the lack of good adhesion to Li electrodes (high-modulus materials often do not afford good adhesion) significantly increases interfacial resistance during cycling.⁷ Moreover, the electrochemical stability window of ceramic electrolytes is very narrow.⁸

The use of *solid polymer electrolytes* (SPEs) represents the ultimate solution due to the chemical stability of these materials toward Li metal electrodes and their mechanical resistance to dendrite growth. SPEs have a much better adhesion with electrodes than ceramics, which, along with their good flexibility and scalable fabrication, makes them favorable for battery manufacturing. The first observation of ionic conductivity in complexes of lithium salts within linear poly(ethylene oxide) (PEO) appeared in 1973 in *Polymer*, while its application in a battery cell was validated several years later.⁹ Since then, PEO has been the subject of extensive studies owing to its ability to solvate a wide variety of lithium salts; the ethylene oxide (EO) units have a strong affinity for Li^+ , while their high chain flexibility and low glass transition temperature promotes fast ion transport (Figure 1a). It is widely accepted that ion conduction occurs in the amorphous PEO phase and that ion diffusion is coupled with the PEO dynamics (Figure 1a, top).¹⁰ At temperatures below the crystalline melting temperature of PEO ($T_m \approx 60^\circ\text{C}$, for PEO molecular weight $M_w > 1 \text{ kg/mol}$), the electrolyte is solid with $G' \approx 0.1 \text{ GPa}$ (i.e., close to the required, Figure 1b), but ion

conductivity at room temperature is $\sigma \approx 10^{-6}\text{--}10^{-8} \text{ S/cm}$, i.e., several orders of magnitude lower than what is required for practical applications (Figure 1c). At temperatures $T > T_m$, the volume fraction of the amorphous, conductive PEO phase increases, Li^+ may transport throughout the whole material (Figure 1a, bottom), and the ionic conductivity can be as high as 10^{-3} S/cm (Figure 1c); nevertheless, the melting of PEO crystals results in a modulus of $1\text{--}10 \text{ MPa}$ (Figure 1b) and does not meet the criterion for reduced dendrite formation. Unfortunately, in homogeneous polymer materials, any attempt to improve conductivity via faster polymer motions results in a decrease in stiffness.

At low molecular weights, with unentangled linear PEO homopolymer electrolytes, ion diffusion occurs via the diffusion of the entire PEO chain with the coordinated ion. With increasing PEO molecular weight, entanglements start to occur between polymer chains; ion diffusion is primarily mediated by segmental dynamics and Li^+ hopping between adjacent ether oxygen atoms with the processes of breaking/forming lithium–oxygen (Li–O) bonds (fluctuation driven diffusion). Both mechanisms should occur in polymer systems with the relative importance to depend on the molecular weight. As a result, at molecular weight higher than 1–2 kg/mol, the ionic conductivity is independent of the PEO chain length (Figure 1d). It is important to point out that ion conductivity depends strongly on the lithium salt concentration and has a nonmonotonic behavior with lithium salt weight fraction (orange data, left axis in Figure 1e). This is the result of two competing factors: on one hand, ionic conductivity increases with lithium salt weight fraction as the free ion concentration increases (light blue triangles, right axes

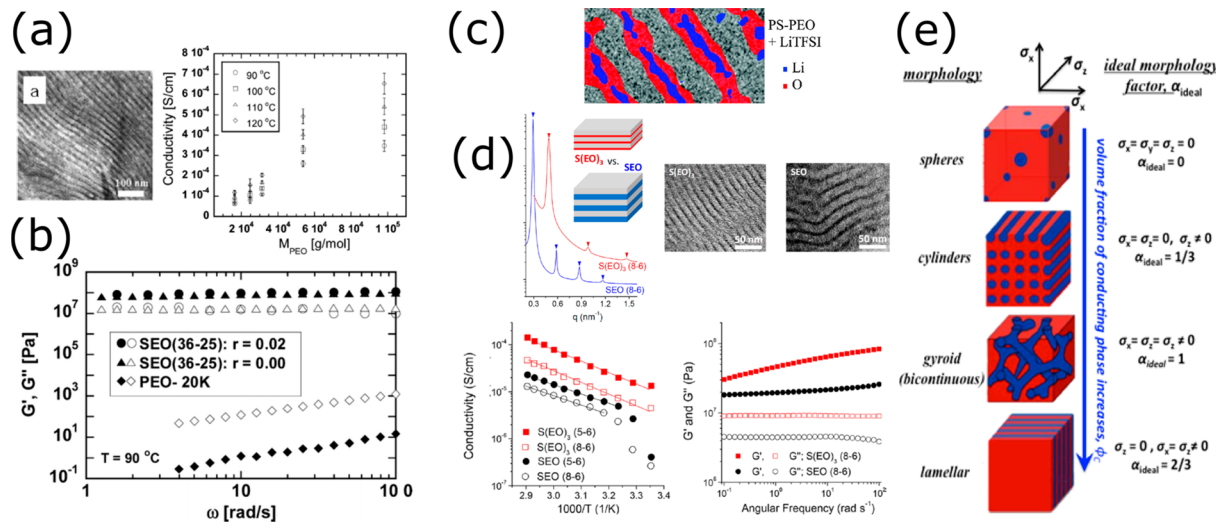


Figure 2. (a) TEM images of a lamellar-forming PS-*b*-PEO block copolymer (PEO phase is darkened by RuO₄) (left) molecular weight dependence of the ionic conductivity of PS-*b*-PEO block copolymer with [Li⁺]/[EO] = 0.02, at selected temperatures. (b) Storage (solid symbols) and loss (open symbols) moduli of linear of PS-*b*-PEO block copolymer at different [Li⁺]/[EO] and the corresponding behavior of linear PEO. (c) LiTFSI distribution contour map in a lamellar-forming BCP measured by energy-filtered TEM; the blue region indicates the localization of the Li in the middle of the PEO lamellar (red region), while gray regions represent the PS phase (Reprinted from the work of Gomez et al.,¹⁷ Copyright 2009. American Chemical Society). (d) scattering profiles and corresponding TEM images (top), temperature dependence ion-conductivity (bottom left) and frequency-dependence storage (solid symbols) and loss (open symbols) moduli of PS-*b*-PEO and PS-*b*-(PEO)₃ having nominally the same molecular weight at [EO]/[Li] = 0.06 (Reprinted from the work of Lee et al.,¹⁸ Copyright 2018. American Chemical Society). (e) Dependence of the ideal morphology factor on the morphology.

in Figure 1e), and on the other hand, due to the polymer–ion interactions, polymer dynamics decrease monotonically with increasing salt concentration (dark blue squares, right axes in Figure 1e); that tends to decrease ion conductivity (Figure 1e).

In homogeneous polymer materials, like pure PEO-based electrolytes, ion motion/transport is coupled with segmental dynamics, and any attempt to improve conductivity via faster polymer motions and/or melting of crystals results in a decrease in stiffness.¹⁰ The “state-of-the-art” approach to decouple these two antagonistic parameters is the generation of *multi-phase nanostructured polymer electrolytes*, where one phase conducts ions (that needs to be soft/mobile phase needed for fast ion motion), while the insulating glassy phase imparts the desired mechanical properties.^{12,13} It is important to point out that the addition of inorganic particles (hybrid polymer nanocomposite electrolytes) offers a facile route to imparting needed materials characteristics and has attracted considerable interest for the synthesis of high-performance solid polymer electrolytes.^{14,15} However, despite the developments reported across a rich breadth of polymer electrolytes systems, the best performing electrolytes with $G' \sim \text{GPa}$ still have at least two orders of magnitude lower ionic conductivities than what is required when their mechanical properties are achieved.

2. BLOCK COPOLYMER ELECTROLYTES

A cost-effective, robust, and scalable way to generate complex multidomain morphologies involves the self-assembly of block copolymers (BCPs). The most basic version of a copolymer is a linear diblock copolymer in which two chemically distinct chains, or blocks, are linked end-to-end. The classic battle between entropy and enthalpy, coupled with the geometric constraints on phase separation, cause these materials to self-assemble into nanostructured morphologies with length scales on the order of 5–100 nm controlled by their molecular

characteristics.¹⁶ These morphologies include spheres arranged on a body-centered-cubic lattice, hexagonally packed cylinders, bicontinuous gyroid networks, and stacked lamellae depending on the composition of the block copolymer. At high enough temperatures, entropy dominates, causing the two blocks to homogeneously mix in a disordered phase; the nature of concentration fluctuations in the disordered phase has been studied in considerable detail.¹⁶ The self-assembly behavior and resultant structure is controlled by the volume fraction of one component f and the degree of segregation χN ; χ is the Flory–Huggins interaction parameter, which parametrizes the thermodynamic compatibility between the two blocks, and N is the overall degree of polymerization. By tuning these parameters appropriately, it is possible to obtain nanostructured materials that combine the properties of the constituent blocks. This has led researchers to use block copolymers as solid membranes for selective transport of various species, typically with one transporting block and one structural block.

Microsegregated PEO-based copolymer electrolytes are currently the most commonly studied nanostructured materials in all-polymer nanostructured solid electrolytes. The earlier work on triblock copolymer electrolytes was reported by Giles group in 1987. The triblock copolymer was based on a styrene–butadiene–styrene ABA triblock copolymer having pendant, short PEO chains grafted onto the B block. The PEO volume fraction in the polymer was controlled by varying either the number of pendant groups or their molecular weight. In the absence of any morphological and mechanical analysis, an ion conductivity of $\sigma \approx 10^{-6} \text{ S/cm}$ was reported at room temperature. In 1999, Mayes et al. proposed the use of comb diblock copolymer, where the conducting block was composed of a poly(methacrylate) backbone grafted with short PEO side chains (POEM). The idea was that low-molecular weight PEO chains, grafted to synthetic backbone, would have both fast

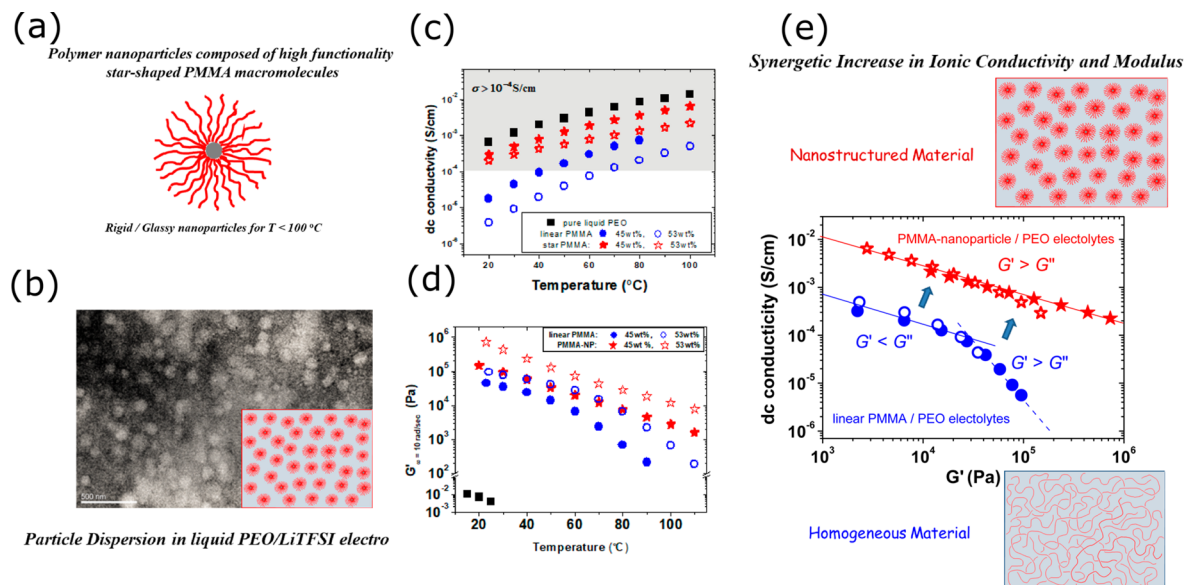


Figure 3. (a) Schematic of the PMMA-NP composed of high functionality star-shaped PMMA molecular. (b) TEM micrographs of a 45 wt % PMMA-NP/linear PEO-0.55K blend; the PMMA nanoparticles appear bright (negative staining) after staining with RuO₄ for 5 min, since RuO₄ preferentially stains the PEO phase. The inset in (b) shows a schematic of the organization of PMMA nanoparticles (red star-shaped particles) within a linear PEO electrolyte (blue background). (c) The direct-current (dc) conductivity as a function of temperature for the pure PEO (black squares), the 45 and 53 wt % linear LPMMA/PEO blends (filled and open blue circles, respectively), and the 45 and 53 wt % PMMA-NP/PEO blends (filled and open red stars, respectively); the gray region highlights the $\sigma > 10^{-4}$ S/cm regime. (d) Storage modulus G' as a function of temperature (obtained from the frequency sweeps in the linear regime for $\omega = 10$ rad/s) for the 45 and 53 wt % blends of linear PMMA (blue filled and open circles for the 45 and 53 wt %, respectively) and PMMA-NP (red filled and open stars for the 45 and 53 wt %, respectively). (e) The dc conductivity vs storage modulus for the 45 wt % (open symbols) and 53 wt % (filled symbols) blends for linear PMMA/PEO (blue circles, homogeneous materials) and PMMA-NP/PEO (red stars, nanostructured materials) solid polymer electrolyte blends. The lines were drawn as a guide (Reprinted from the work of Glynnos et al.²⁶ Copyright 2018. American Chemical Society).

dynamics and suppressed crystallization, favoring high ionic conductivity.¹⁹ By synthesizing a variety of different POEM-based diblock copolymers, where the second block was either poly(lauryl methacrylate) (PLMA, $T_g \approx -35$ °C), poly(*n*-butyl methacrylate) (PnBMA, $T_g \approx -40$ °C), or poly(methyl methacrylate) (PMMA, $T_g \approx -100$ °C), they showed that the highest conductivity is obtained when the POEM block is attached to the soft, rubbery PLMA block, rather than to a glassy PMMA block. SPEs with $\sigma \approx 5 \times 10^{-5}$ S/cm and $G' \approx 0.5$ MPa were reported for the POEM-*b*-PLMA block copolymer. On the basis of the same POEM conducting block, Niitani et al. showed that the ionic conductivity and mechanical strength vary in opposite way in polystyrene-*b*-poly(ethylene glycol methacrylate)-*b*-polystyrene (PS-*b*-POEM-*b*-PS) comb triblock copolymers and depend on the PEO weight fraction.²⁰ At 30 °C, when the PEO content exceeded 80%, an ionic conductivity of $\sim 10^{-4}$ S/cm was reported but with a very poor mechanical strength as the soft, liquid-like, low molecular weight (M_w) PEO grafted chains dominated the average mechanical response of the polymer electrolyte.

Balsara's group²¹ has extensively studied the linear PS-PEO diblock copolymer-based electrolytes. Unexpectedly for what it was known for PEO-based electrolytes, in PS-*b*-PEO electrolytes doped with lithium bis(trifluoromethanesulfonyl) imide (LiTFSI) the ion conductivity was shown to increase with the molecular weight of the PEO block; something that was recently verified and predicted also theoretically.²² Balsara's group explained this behavior in terms of the existence of a "dead zone" for ion transport next to PS/PEO interface (Figure 2c).¹⁷ As the molecular weight of the PEO block

increases, the volume fraction of the "dead zone" decreases, and ion-conductivity increases. A PS/PEO molar ratio around unity (i.e., in lamellar forming electrolytes) provides the best balance between mechanical strength and ionic conductivity (Figure 2a,b). At temperatures below the glass transition temperature of the PS, that is, for $T < 100$ °C, $G' \approx$ GPa (Figure 2b). Despite the good mechanical properties of PS-*b*-PEO/LiTFSI electrolytes for a wide range of temperatures, the ion conductivity at room temperature was $\sim 10^{-7}$ S/cm (Figure 2a), that is, 3 orders of magnitude lower than what is required for any practical application. Only at temperatures higher than ~ 80 °C, that is, at temperatures above the melting of the PEO crystals, $\sigma(T) \approx 10^{-4}$ S/cm in the best-performing linear BCP/Li salt electrolyte.

Park et al. showed that Li⁺ transport in PEO/PS copolymers may be improved by employing a mikto-arm star architecture composed of three PEO arms connected to one PS chain, that is, PS(PEO)₃.¹⁸ A simultaneous enhancement in both the ionic conductivity and mechanical strength was reported in PS-(PEO)₃ when compared to their PS-*b*-PEO analogues (Figure 2d). Because of the star-shaped architecture of PS(PEO)₃ and associated geometrical constraints, PEO crystallization was significantly reduced giving rise to room-temperature conductivities an order of magnitude higher compared to the corresponding PS-*b*-PEO. Geometrical constraints imposed by the star-shaped macromolecular architecture of PS(PEO)₃ showed the reduction of the segregation strength of PS and PEO block giving rise to a notably smaller domain spacing for PS(PEO)₃ compared to the linear analogues.

3. NANOSTRUCTURING ALL-POLYMER ELECTROLYTES—BEYOND BLOCK COPOLYMERS

To further articulate the need for nanostructured solid polymer electrolytes with designing rules beyond the use of micro-segregated block copolymers, a short overview of the factors that affect the ion conductivity in block copolymer materials and limit their realization in solid polymer electrolytes is provided below.

Research in the field has revealed that one of the main drawbacks for the realization of block copolymer electrolytes is the formation of grains across the thickness of an electrolyte's membrane. When Li^+ diffuses between electrodes, the corresponding ion conduction has two terms: the intragrain and intergrain transport. Intragrain transport indicates conduction within grain boundaries, while intergrain transport describes the connectivity of conducting pathways across grain boundaries. For intragrain ion transport, domain orientation and dimensionality of the conducting pathway are the key factors. In BCP systems, the intragrain ionic conductivity $\sigma(T)$ can be expressed as¹⁰

$$\sigma(T) = a\phi_c\sigma_{\text{cond}}(T) \quad (1)$$

where a is the morphology factor that accounts for grain boundary effects and the geometry and interconnectivity of the conducting phase, ϕ_c is the volume fraction of the conducting phase, and $\sigma_{\text{cond}}(T)$ is the intrinsic conductivity of the conducting phase. Theoretical work of Sax and Ottino on transport through heterogeneous media enabled calculations of the dependence of a on electrolyte morphology.²³ We refer to these calculated values as a_{ideal} , as they do not take into account grain boundaries effects. The values of a_{ideal} for the typical morphologies of copolymers are presented in Figure 2e. The conducting phase (shown in blue) is the minority block, while the majority phase is the insulating hard block (shown in red). For the sphere morphology, $a_{\text{ideal}} = 0$, since there is no effective conducting pathway, $\sigma_x = \sigma_z = \sigma_y = 0$. For cylinders $a_{\text{ideal}} = 1/3$, and for lamellae $a_{\text{ideal}} = 2/3$, because on average only one- or two-thirds of the grains will contribute to the ion transport in a specific direction, respectively. For the bicontinuous morphology (like gyroid) $a_{\text{ideal}} = 1$ as intragrain ion conduction is isotropic and occurs in all directions. Nevertheless, due to grain boundaries effects and intergrain ion transport, the experimentally determined morphology factors, a , of BCP-based electrolytes are significantly less than a_{ideal} , that is, $a < a_{\text{ideal}}$ (see Table 1 in ref 24). Cylinders forming BCP electrolytes are strongly affected by grain orientation angles and discontinuities in the conducting domains, and a has been estimated to be ~ 0.03 , that is, an order of magnitude lower than the theoretical intragrain transport $a_{\text{ideal}} = 0.33$. Notably, the morphology factors obtained for the gyroid (bicontinuous) morphologies are much smaller than unity and comparable with lamellar-forming BCP electrolytes.

Phase discontinuity across grains demonstrates the necessity for the synthesis of copolymer domains with long-range order as well as isotropic, highly interconnected three-dimensional (3D) conducting pathways. Eq 1 dictates that, for the highest possible $\sigma(T)$ in linear block copolymer electrolytes, the conducting block, ϕ_c , should be the majority block. This would also enable the sphere morphology composed of the insulating block (minority block) (Figure 3), while it should be $a = a_{\text{ideal}} = 1$ as the conducting phase in an interconnecting 3D matrix with no grain boundaries. Nevertheless, such polymeric

nanostructured materials have poor mechanical properties, as their mechanical behavior is dominated by the soft/rubbery conducting phase,²⁵ and they were abandoned many years ago. Nevertheless, in linear block copolymers an increase of the volume fraction insulating stiff block in an effort to increase the mechanical response of the system would result to a morphology change from spheres to cylinders, a_{ideal} would decrease to $1/3$, and grain boundaries effect will be introduced, that is, $a < a_{\text{ideal}}$. As the diblock copolymer phase diagram dictates, such a morphological transition would occur for a volume fraction of the stiff/insulating phase larger than 0.15–0.2%. Hence, the need for continuous pathways with the conducting domain being the majority, which is not feasible with linear copolymers, where the grain boundary effects are eliminated hold the key for high conductivities.

Recently, in an effort to engineer all-polymer SPEs with a morphology akin to sphere morphology of block copolymers and independent of the volume fraction of the involved phases, that is, not accessible before by linear block copolymers, counterparts we introduced the use of stiff/rigid polymer poly(methyl methacrylate) (PMMA), nanoparticles (PMMA-NP), composed of high-functionality star-shaped PMMA molecules, as additives to liquid polymer PEO/LiTFSI electrolytes.²⁶ To this end, star-shaped polymers with a large number of polymer chains grafted together to a core, can be considered molecules with a colloid-, particle-like character.²⁷ Notably, at temperatures below the T_g of PMMA (~ 110 to 120 °C), the PMMA polymer nanoparticles are glassy/stiff could be used as reinforcing agents that, compared to the widely used inorganic nanoparticles in hybrid composite electrolytes, offer the possibility of enhancing the specific energy of a battery device, since much lighter electrolytes could be synthesized.

It was demonstrated that, when PMMA-NP was added to the liquid polymer electrolyte, both the elastic modulus and the ionic conductivity of the resulting SPE increased compared to the linear blend analogues. In particular, the addition of 53 wt % PMMA nanoparticles resulted in SPEs that exhibited two orders of magnitude higher conductivity and one order of magnitude higher mechanical strength as compared to their linear PMMA blend analogues (Figure 4). At room temperature PMMA-NP/PEO/LiTFSI electrolytes have a $\sigma > 10^{-4}$ S/cm and $G' \approx 1$ MPa, and they outperform the corresponding nanocomposite electrolytes made with the addition of silica NPs.^{28,29} The key to this phenomenon is the morphology of the resulting SPEs: for the linear PMMA/PEO blends a homogeneous, single-phase material was obtained, whereas for the PMMA-nanoparticle/PEO blends, a nanostructured composite material was formed with highly interconnected conducting regions, pure in liquid PEO, as the result of PMMA nanoparticle dispersion within the liquid electrolyte. These differences in morphology resulted in a significant decoupling of conductivity from the mechanical strength for the PMMA-NP/PEO blends, even when the electrolyte was in the solid state.

Lodge, Hilmeyer, and co-workers, using a facile single-pot strategy, reported the synthesis of mechanically robust nanostructured SPEs with bicontinuous morphology with high conductivity that significantly outperformed the best-performing PS-*b*-PEO based electrolytes (Figure 5).³⁰ The synthetic protocol that was followed resulted in bicontinuous, nanostructured solid polymer electrolytes with interconnected and interpenetrating domains of cross-linked PS that provided

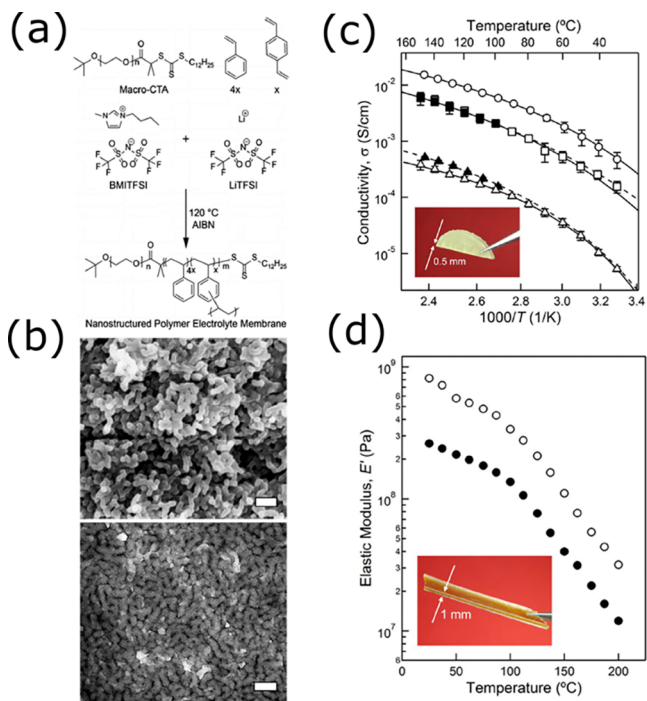


Figure 4. (a) Reaction scheme used to prepare polymerization-induced phase separation polymer electrolyte membranes (PIPS PEMs). (b, top) Scanning electron micrograph of the sample after etching of PEO and BMITFSI with 57 wt % aqueous hydroiodic acid; (b, bottom) transmission electron micrograph of the same sample prior to etching. The PEO/ionic liquid domain appears dark after staining with RuO₄. Both scale bars represent 100 nm. (c) Ionic conductivity as a function of temperature for PEMs prepared with 5 kg mol⁻¹ PEO-CTA (CTA = chain transfer agent). Open symbols: Samples prepared with BMITFSI. Filled symbols: Samples prepared with a 1 M mixture of LiTFSI in BMITFSI. Overall salt concentrations are 5 (\triangle), 7 (\blacktriangle), 21 (\square and \blacksquare), and 40 vol % (\circ). (d) Temperature-dependent linear elastic response of PIPS PEMs prepared with 28 kg mol⁻¹ PEO-CTA and no ionic liquid (\circ) and 21 vol % BMITFSI (\bullet) (Reprinted from the work of Schulze et al.³⁰ Copyright 2014. American Chemical Society).

a modulus of ~ 0.1 GPa, and an ion-conducting phase (PEO domains swollen with IL and doped with lithium bis(trifluoromethanesulfonyl)imide (LiTFSI)) that had a conductivity higher than 10^{-4} S/cm at room temperature. It is interesting to note that, because of the presence of the high glass transition PS-cross-linked network, the SPE could maintain its robustness at temperatures close to 100 °C with significantly higher conductivity.

Recently, we proposed a facile new approach for the synthesis of all-polymer nanostructured solid electrolytes that exhibit an unprecedented combination of high modulus and ionic conductivity at room temperature.³¹ Novel nanostructured polymer particles, composed of miktoarm stars with a very large number of arms (functionality) of ion conducting poly(ethylene oxide) (PEO) arms that complement stiff insulating polystyrene arms, PS, $((\text{PS})_n(\text{PEO})_n)$, where $n = 30$ the number of arms), were synthesized and added to a low molecular weight PEO doped with LiTFSI. The addition of 44 wt % $(\text{PS})_{30}(\text{PEO})_{30}$ in liquid PEO/LiTFSI electrolyte resulted in SPEs with a shear modulus of $G' \approx 0.1$ GPa and ion conductivity $\sigma \approx 10^{-4}$ S/cm, at room temperature. The SPEs showed a strong decoupling between the mechanical behavior and the ionic-conductivity as G'

remains fairly constant for temperatures up to the glass transition temperature of the PS blocks, while the conductivity monotonically increased to reach $\sigma \approx 10^{-2}$ S/cm at $T = 100$ °C. Key to their performance is their morphology that stems from the ability of the $(\text{PS})_{30}(\text{PEO})_{30}$ nanoparticles to self-assemble in highly interconnected structures within the liquid electrolytes host. Harmandaris and co-workers showed that these $(\text{PS})_n(\text{PEO})_n$ miktoarm star-shaped polymers, due to the unfavorable interactions between the PS and PEO arms, form internally nanostructured particles whose final morphology and shape critically depend on the number and length of the arms; while the miktoarm stars with functionalities lower than 16 nanosegregate into two main regions, resembling a structure akin to Janus particles, the 32-arm stars form multi-patchy nanoparticles.³² As a result of their intramolecular nanostructured morphology, when such nanostructured particles are added to a liquid PEO electrolyte, specific interactions with the liquid electrolyte are activated, directing their self-assembly into highly interconnected structures and promoting the decoupling of the antagonistic properties of conductivity and mechanical strength.³³

4. SINGLE-ION NANOSTRUCTURED SOLID ALL-POLYMER ELECTROLYTES

Conventional SPEs are formed by dissolving Li salt in a polymer host that solvates the lithium salt. Such systems are dual conductors as both anions and cations are mobile. In PEO-based electrolytes, the fraction of conductivity from the cations (Li^+ transference number, t_{Li}^{+}) is only a small fraction of the overall conductivity (~1/5). The low transference number occurs due to the strong preferential solvation of Li^+ over its counteranion, resulting in a bulky solvation shell around Li^+ compared to that of typical anions.³⁴ The large contribution from the anions leads to a strong concentration gradient as anions accumulate at the electrode, leading to deleterious effects such as concentration polarization. This greatly increases cell resistance, limits cell lifetime, and promotes fast dendrite growth that ultimately limits power delivery.

As early as 1994, Doyle, Fuller, and Newman demonstrated the importance of using single-ion electrolytes for batteries applications, that is, the use of electrolytes with t_{Li}^{+} close to unity. It was demonstrated that a single-ion electrolyte could perform better when incorporated to a battery cell when compared to a dual-ion electrolyte having an order of magnitude larger ionic conductivity.³⁵ Even a modest improvement in t_{Li}^{+} , that is, from 0.3, found in simple dry PEO-based electrolytes, to $t_{\text{Li}}^{+} \approx 0.7$, would allow much higher charge/discharge rates, of paramount importance in electric vehicles applications.³⁴ To this end, the most common strategy for the synthesis of polymer electrolytes with t_{Li}^{+} close to unity is the tethering and immobilization of anions to the polymer backbone. Among the various systems that have been developed, including acrylate-, sulfonate-, and borate-based polymers, polymers containing anions of (trifluoromethanesulfonyl)imide (TFSI⁻) have attracted considerable attention over the last years due to the binding affinity with Li^+ , possess highly delocalized negative charge over large conjugate structure (four oxygen and one nitrogen) and good plasticizing ability for the polymer backbone.³⁶⁻³⁹

Armand and co-workers were the first to report the synthesis of polystyrene-*b*-poly(ethylene oxide)-*b*-polystyrene triblock copolymer, wherein lithium bis(trifluoromethane) sulfonamide

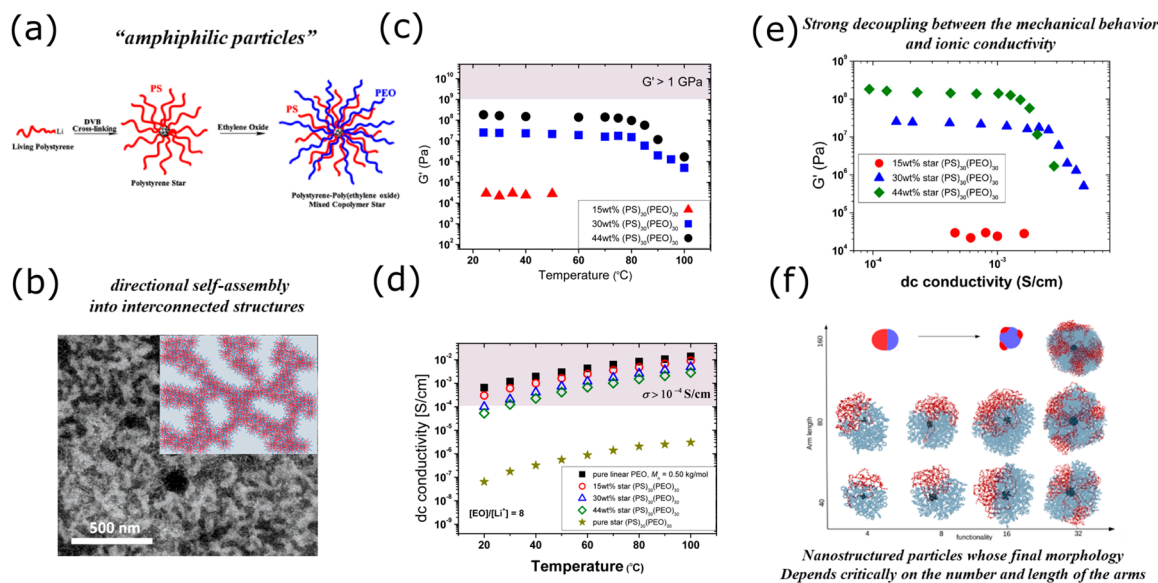


Figure 5. (a) Schematic of the DVB synthetic route for the synthesis of PS (red arms) and PEO (blue arms) asymmetric miktoarm star-shaped copolymers. (b) TEM micrographs at 30 wt % (PS)₃₀(PEO)₃₀/linear PEO with $M_w = 0.55 \text{ kg/mol}$ blend; the inset in (b) is a schematic that represents the organization of (PS)₃₀(PEO)₃₀ particles within the PEO host. The PEO domains appear dark after staining with RuO₄ for 5 min. (c) G' as a function of temperature in the linear regime at $\omega = 10 \text{ rad/s}$ for the 15, 30, and 44 wt % (PS)₃₀(PEO)₃₀ (red triangles, blue squares, and black circles, respectively). (d) The ion conductivity as a function of temperature for pure linear oligomeric PEO (black squares), pure (PS)₃₀(PEO)₃₀ (dark yellow stars), and blends of 15, 30, and 44 wt % (PS)₃₀(PEO)₃₀ (red circles, blue triangles, and green rhombus, respectively); the gray region highlights the $\sigma \geq 10^{-4} \text{ S/cm}$ area. (e) Storage modulus vs dc ionic conductivity for the 15, 30, and 44 wt % (PS)₃₀(PEO)₃₀ blends (red circles, blue triangles, and green rhombus, respectively) (Reprinted from the work of Glynnos et al.³¹ Copyright 2017. American Chemical Society). (f) Scheme from atomistic simulation of nanosegregated miktoarm star particles in vacuum at 400 K. The gray central region represents the star core, PEO arms are shown in red, and PS arms are shown in blue. The atoms of PS monomers are transparent for better visibility of PEO block segregation (Reprinted from the work of Bacova et al.³² Copyright 2014. American Chemical Society).

(LiTFSI) was covalently linked to styrene units in the PS block (PSLiTFSI), PSLiTFSI-*b*-PEO-*b*-PSLiTFSI.³⁷ Different tri-block copolymers were synthesized; the M_w of PEO remained constant at 35 kg/mol, while the M_w of each of the two PSLiTFSI blocks was varied from 1.85 kg/mol (resulting to a $[\text{EO}]/[\text{Li}^+] = 69$) to 13.2 kg/mol ($[\text{EO}]/[\text{Li}^+] = 10$). The polymer electrolytes with PSLiTFSI M_w of 4.75 and 16 kg/mol showed the maximum conductivity: $\sigma \approx 10^{-5} \text{ S/cm}$ at 60°C, with $t_{\text{Li}}^+ = 0.85$ and fairly good mechanical properties (10 MPa at 40 °C). Despite the good electrochemical stability window (up to 5 V vs Li⁺/Li) and improved cycling performance in lithium metal battery prototypes, due the PEO crystallization, at room temperature the ionic conductivity was $\sigma \approx 10^{-7} \text{ S/cm}$, that is, several orders of magnitude lower than that required for practical applications. Balsara and co-workers synthesized various PEO-*b*-PSLiTFSI single-ion block copolymers and showed that the crystallization PEO at low temperatures (i.e., at $T < T_c$ of PEO) drives the formation of lamellar morphology, lowering the degree of ion dissociation, as Li⁺ ions are trapped in the form of ionic clusters with the PS domains, resulting in very low conductivity (Figure 6a,b).^{38,39} At temperatures above PEO melting, the material goes to a disordered phase, and Li⁺ ions are efficiently released and dissociated from the clusters, accompanying a several orders of magnitude increase in ion conductivity. Nevertheless, in the conductivity phase the material transforms from a rigid solid to a disordered viscoelastic liquid.

In a recent work, Balsara's group proposed an alternative approach for the synthesis of single-ion nanostructured polymer materials based on the addition of functionalized silsesquioxane nanoparticles (salty nanoparticles) to micro-

phase-separated PS-*b*-PEO copolymers.⁴⁰ The POSS-PSLiTFSI nanoparticles were mixed at different loadings with PS-*b*-PEO and SPEs with $r = [\text{Li}]/[\text{EO}] = 0.02, 0.05, 0.085$, and 0.10 were synthesized. Because of the miscibility of the PSLiTFSI ligands with PEO, the salty nano-particles were preferentially located in the PEO-rich phase, as it was revealed by high-resolution dark-field scanning transmission electron microscopy (TEM)/energy-dispersive X-ray spectroscopy (EDS) measurements (Figure 6d). Regardless of the temperature, the maximum ion conductivity was measured for $[\text{Li}]/[\text{EO}] = 0.085$ (i.e., for 28.4 wt % of salty POSS-PSLiTFSI nanoparticles). At 60 °C, $\sigma = 1 \times 10^{-6} \text{ S/cm}$, while at room temperature, $\sigma = 8 \times 10^{-8} \text{ S/cm}$; that is, a factor of 10 lower than PSLiTFSI-*b*-PEO-*b*-PSLiTFSI and PEO-*b*-PSLiTFSI.^{37–39} In contrast to the single-ion PEO-*b*-PSLiTFSI electrolytes, POSS-PSLiTFSI/PS-*b*-PEO remained nanostructured and rigid solid even in the conducting state, that is, at temperature above the melting temperature of PEO. This was attributed to the increasing segregation strength of PS and PEO domains with the addition of the salty nanoparticles. Furthermore, the presence of POSS-PSLiTFSI particles in the PEO-rich domain results in $t_{\text{Li}}^+ = 0.98$, that is, very close to unity and larger than the reported $t_{\text{Li}}^+ = 0.85$ for the PSLiTFSI-*b*-PEO-*b*-PSLiTFSI single-ion electrolytes.

5. CONCLUSIONS AND OUTLOOK

In conclusion, we reviewed the recent progress in nanostructured all-polymer electrolytes focusing on the solid polymer electrolytes that could simultaneously have high ionic conductivity Li⁺ and transference number. As is highlighted in this Mini Review, it is necessary to design

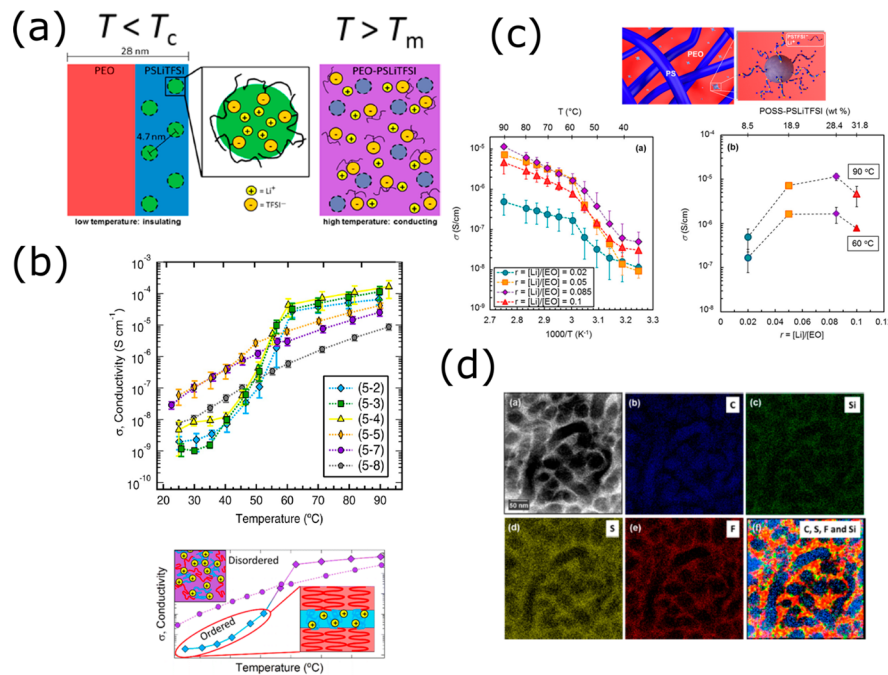


Figure 6. (a) Schematic of PEO-*b*-PSLiTFSI single-ion electrolytes at temperatures below PEO melting temperature ($T < T_m$, left part) and at $T > T_m$ (right part). At $T < T_m$, ions are clustered and trapped within the PEO, microphase separated region. At $T > T_m$ the electrolyte is disordered, amorphous, ions are dissolved, and the Li^+ ion is mobile (Reprinted from the work of Inceoglu et al.³⁸ Copyright 2014. American Physical Society). (b) Ionic conductivity of PEO-*b*-PSLiTFSI single-ion copolymers at various temperatures; the bottom image is the effect of PSLiTFSI molecular weight on the morphology and ion conductivity of the single-ion electrolytes (Reprinted from the work of Rojas et al.³⁹ Copyright 2015. American Physical Society). (c) Single-ion electrolytes systems based on salty POSS-PSLiTFSI nanoparticles (top right schematic) blended with PEO-*b*-PS copolymers (top left schematic). The bottom plots show the temperature dependence of the ion conductivity of POSS-PSLiTFSI/PEO-*b*-PS single-ion electrolytes at different nanoparticles loadings (right) and the effect of nanoparticles weight fractions and corresponding $[\text{Li}]/[\text{EO}]$ on the ionic conductivity at 60 and 90 °C. (d) STEM and element maps PSLiTFSI/PEO-*b*-PS single ion electrolytes with $[\text{Li}]/[\text{EO}] = 0.085$ (Reprinted from the work of Villaluenga et al.⁴⁰ Copyright 2017. American Physical Society).

novel polymer electrolytes using designed rules beyond that of microphase-segregated PEO block copolymer-based electrolytes. Great efforts are still needed to overcome these obstacles and include the following:

- The very low room-temperature ionic conductivity of PEO-based electrolytes, several order of magnitudes lower than what is required for practical application, is still an obstacle for their application as room-temperature Li metal batteries. Novel polymer materials with designing rules beyond the microphase-segregated PEO block copolymer-based electrolytes should be systematically explored. This need stems from the fact that, in such systems, the synthesis of electrolytes with interconnected phase in the macroscale is very challenging, and along with the PEO crystallization results in room-temperature conductivities that are several orders of magnitude lower than what is required for practical applications. The findings summarized in the Mini Review suggest that there are a couple of very promising pathways toward the synthesis of all-polymer solid polymer electrolytes with ion conductivity and mechanical properties close to the requirements based on nanostructured polymer nanoparticles as additives to liquid polymer electrolytes (Figure 5) on polymerization-induced phase separation method (Figure 4). Systematic studies toward macromolecular optimization of the aforementioned approaches may hold the key for their realization in lithium metal batteries.

- Improving the Li ion transference number is an important task, since it can simultaneously reduce polarization, suppress Li dendrite growth, and extend the lifetime of lithium metal batteries. We expect an increasing effort to chemically and structurally modify existing polymer chemistries in dual-ion conductors to enhance negative charge delocalization. By doing so, both room-temperature conductivities will be enhanced, and single-ion electrolytes with $\sigma > 10^{-5}$ S/cm could be efficiently incorporated in safe to use lithium metal batteries.

Considering the rapidly growing academic and industrial interests in developing solid polymer electrolytes for solid-state lithium-based batteries, it is reasonable to expect important breakthroughs in the near future.

AUTHOR INFORMATION

Corresponding Authors

Emmanouil Glynnos – Institute of Electronic Structure and Laser, Foundation for Research and Technology—Hellas, 71110 Heraklion, Crete GR, Greece; orcid.org/0000-0002-0623-8402; Email: eglynnos@iesl.forth.gr

Georgios Sakellariou – Department of Chemistry, National and Kapodistrian University of Athens, 15771 Athens, Greece; orcid.org/0000-0003-2329-8084; Email: gsakellariou@chem.uoa.gr

Author

Christos Pantazidis – Department of Chemistry, National and Kapodistrian University of Athens, 15771 Athens, Greece

Complete contact information is available at:

<https://pubs.acs.org/10.1021/acsomegajournal.9b04098>

Notes

The authors declare no competing financial interest.

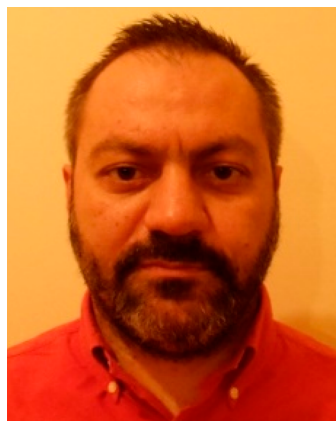
Biographies

Emmanouil Glynnos studied physics at the University of Patras, and he received his PhD in 2007 in polymer physics at the University of Edinburgh. Until 2012, he was a postdoctoral research associate at the Department of Material Science and Engineering at the University of Michigan, working on the effect of macromolecular architecture on the physical properties of polymers at surfaces and interfaces. He was subsequently appointed as a Research Investigator at the University of Michigan at the Center for Solar and Thermal Energy Conversion, where his research was focused in addressing important scientific challenges associated with the structure–property relations and correlations of the morphology of the device active layer on the nanometer scale to the electrical and optical properties, the charge photogeneration, and overall performance of these systems. Since 2015 he is a Research Scientist at FORTH/IESL, where the objective of his current research is to develop a fundamental understanding of, and controlling via macromolecular engineering, the structure and properties of nanostructured polymer materials that can be used as solid electrolytes in lithium–metal batteries and electrochromic devices and as active layers in organic photovoltaics.



Christos Pantazidis studied Chemistry at the National and Kapodistrian University of Athens. In 2015 he joined Prof. Sakellariou's group, where he received his Master's degree in polymer science, specializing in anionic polymerization techniques. Since 2018

he is a PhD candidate, and his research interests are focused on synthesizing polymer electrolytes.



Georgios Sakellariou is an Associate Professor at the Department of Chemistry at the National and Kapodistrian University of Athens. His current recent interests include the synthesis of polymers with complex macromolecular architectures, surface-initiated polymerizations, polymer nanocomposites, and solution and bulk properties of nanostructured materials.

ACKNOWLEDGMENTS

This research has been cofinanced by the European Union and Greek national funds through the Operational Program Competitiveness and innovation, under the call RESEARCH – CREATE – INNOVATE (Project No. T1EΔK-02576).

REFERENCES

- (1) Bruce, P. G.; Freunberger, S. A.; Hardwick, L. J.; Tarascon, J. M. Li-O₂ and Li-S Batteries with High Energy Storage. *Nat. Mater.* **2012**, *11*, 19–29.
- (2) Armand, M.; Tarascon, J. M. Building Better Batteries. *Nature* **2008**, *451*, 652–657.
- (3) Lin, D.; Liu, Y.; Cui, Y. Reviving the Lithium Metal Anode for High-Energy Batteries. *Nat. Nanotechnol.* **2017**, *12*, 194–206.
- (4) Bouchet, R. Batteries. A Stable Lithium Metal Interface. *Nat. Nanotechnol.* **2014**, *9*, 572–573.
- (5) Tarascon, J. M.; Armand, M. Issues and Challenges Facing Rechargeable Lithium Batteries. *Nature* **2001**, *414*, 359–367.
- (6) Monroe, C.; Newman, J. The Impact of Elastic Deformation on Deposition Kinetics at Lithium/Polymer Interfaces. *J. Electrochem. Soc.* **2005**, *152*, A396–A404.
- (7) Stone, G. M.; Mullin, S. A.; Teran, A. A.; Hallinan, D. T.; Minor, A. M.; Hexemer, A.; Balsara, N. P. Resolution of the Modulus versus Adhesion Dilemma in Solid Polymer Electrolytes for Rechargeable Lithium Metal Batteries. *J. Electrochem. Soc.* **2012**, *159*, A222–A227.
- (8) Zhu, Y. Z.; He, X. F.; Mo, Y. F. Origin of Outstanding Stability in the Lithium Solid Electrolyte Materials: Insights from Thermodynamic Analyses Based on First-Principles Calculations. *ACS Appl. Mater. Interfaces* **2015**, *7*, 23685–23693.
- (9) Fenton, D. E.; Parker, J. M.; Wright, P. V. Complexes of Alkali-Metal Ions with Poly(ethylene oxide). *Polymer* **1973**, *14*, 589–589.
- (10) Hallinan, D. T.; Balsara, N. P. Polymer Electrolytes. *Annu. Rev. Mater. Res.* **2013**, *43*, 503–525.
- (11) Zardalidis, G.; Ioannou, E.; Pispas, S.; Floudas, G. Relating Structure, Viscoelasticity, and Local Mobility to Conductivity in PEO/LiTf Electrolytes. *Macromolecules* **2013**, *46*, 2705–2714.
- (12) Arico, A. S.; Bruce, P.; Scrosati, B.; Tarascon, J. M.; Van Schalkwijk, W. Nanostructured Materials for Advanced Energy Conversion and Storage Devices. *Nat. Mater.* **2005**, *4*, 366–377.
- (13) Cho, B. K.; Jain, A.; Gruner, S. M.; Wiesner, U. Mesophase structure-mechanical and ionic transport correlations in extended amphiphilic dendrons. *Science* **2004**, *305*, 1598–1601.

- (14) Croce, F.; Appetecchi, G. B.; Persi, L.; Scrosati, B. Nanocomposite Polymer Electrolytes for Lithium Batteries. *Nature* **1998**, *394*, 456–458.
- (15) Agrawal, A.; Choudhury, S.; Archer, L. A. A highly Conductive, Non-Flammable Polymer-Nanoparticle Hybrid Electrolyte. *RSC Adv.* **2015**, *5*, 20800–20809.
- (16) Fredrickson, G. H.; Liu, A. J.; Bates, F. S. Entropic Corrections to the Flory-Huggins Theory of Polymer Blends - Architectural and Conformational Effects. *Macromolecules* **1994**, *27*, 2503–2511.
- (17) Gomez, E. D.; Panday, A.; Feng, E. H.; Chen, V.; Stone, G. M.; Minor, A. M.; Kisielowski, C.; Downing, K. H.; Borodin, O.; Smith, G. D.; Balsara, N. P. Effect of Ion Distribution on Conductivity of Block Copolymer Electrolytes. *Nano Lett.* **2009**, *9*, 1212–1216.
- (18) Lee, D.; Jung, H. Y.; Park, M. J. Solid-State Polymer Electrolytes Based on AB₃-Type Miktoarm Star Copolymers. *ACS Macro Lett.* **2018**, *7*, 1046–1050.
- (19) Soo, P. P.; Huang, B. Y.; Jang, Y. I.; Chiang, Y. M.; Sadoway, D. R.; Mayes, A. M. Rubbery Block Copolymer Electrolytes for Solid-State Rechargeable Lithium Batteries. *J. Electrochem. Soc.* **1999**, *146*, 32–37.
- (20) Niitani, T.; Shimada, M.; Kawamura, K.; Dokko, K.; Rho, Y. H.; Kanamura, K. Synthesis of Li⁺ Ion Conductive PEO-PSt Block Copolymer Electrolyte with Microphase Separation Structure. *Electrochim. Solid-State Lett.* **2005**, *8*, A385–A388.
- (21) Singh, M.; Odusanya, O.; Wilmes, G. M.; Eitouni, H. B.; Gomez, E. D.; Patel, A. J.; Chen, V. L.; Park, M. J.; Fragouli, P.; Iatrou, H.; Hadjichristidis, N.; Cookson, D.; Balsara, N. P. Effect of Molecular Weight on the Mechanical and Electrical Properties of Block Copolymer Electrolytes. *Macromolecules* **2007**, *40*, 4578–4585.
- (22) Ganesan, V.; Pyramitsyn, V.; Bertoni, C.; Shah, M. Mechanisms Underlying Ion Transport in Lamellar Block Copolymer Membranes. *ACS Macro Lett.* **2012**, *1*, 513–518.
- (23) Sax, J.; Ottino, J. M. Modeling of Transport of Small Molecules in Polymer Blends - Application of Effective Medium Theory. *Polym. Eng. Sci.* **1983**, *23*, 165–176.
- (24) Villaluenga, I.; Chen, X. C.; Devaux, D.; Hallinan, D. T.; Balsara, N. P. Nanoparticle-Driven Assembly of Highly Conducting Hybrid Block Copolymer Electrolytes. *Macromolecules* **2015**, *48*, 358–364.
- (25) Gray, F. M.; MacCallum, J. R.; Vincent, C. A.; Giles, J. R. M. Novel Polymer Electrolytes Based on ABA Block Copolymerrs. *Macromolecules* **1988**, *21*, 392–397.
- (26) Glynnos, E.; Petropoulou, P.; Mygiakis, E.; Nega, A. D.; Pan, W.; Papoutsakis, L.; Giannelis, E. P.; Sakellariou, G.; Anastasiadis, S. H. Leveraging Molecular Architecture To Design New, All-Polymer Solid Electrolytes with Simultaneous Enhancement in Modulus and Ionic Conductivity. *Macromolecules* **2018**, *51*, 2542–2550.
- (27) Johnson, K. J.; Glynnos, E.; Sakellariou, G.; Green, P. Dynamics of Star-Shaped Polystyrene Molecules: From Arm Retraction to Cooperativity. *Macromolecules* **2016**, *49*, 5669–5676.
- (28) Srivastava, S.; Schaefer, J. L.; Yang, Z. C.; Tu, Z. Y.; Archer, L. A. 25th Anniversary Article: Polymer-Particle Composites: Phase Stability and Applications in Electrochemical Energy Storage. *Adv. Mater.* **2014**, *26*, 201–233.
- (29) Schaefer, J. L.; Moganty, S. S.; Yanga, D. A.; Archer, L. A. Nanoporous Hybrid Electrolytes. *J. Mater. Chem.* **2011**, *21*, 10094–10101.
- (30) Schulze, M. W.; McIntosh, L. D.; Hillmyer, M. A.; Lodge, T. P. High-Modulus, High-Conductivity Nanostructured Polymer Electrolyte Membranes via Polymerization-Induced Phase Separation. *Nano Lett.* **2014**, *14*, 122–126.
- (31) Glynnos, E.; Papoutsakis, L.; Pan, W.; Giannelis, E. P.; Nega, A. D.; Mygiakis, E.; Sakellariou, G.; Anastasiadis, S. H. Nanostructured Polymer Particles as Additives for High Conductivity, High Modulus Solid Polymer Electrolytes. *Macromolecules* **2017**, *50*, 4699–4706.
- (32) Bačová, P.; Glynnos, E.; Anastasiadis, S. H.; Harmandaris, V. Nanostructuring Single-Molecule Polymeric Nanoparticles via Macromolecular Architecture. *ACS Nano* **2019**, *13*, 2439–2449.
- (33) Bačová, P.; Foskinis, R.; Glynnos, E.; Rissanou, A. N.; Anastasiadis, S. H.; Harmandaris, V. Effect of Macromolecular Architecture on the Self-assembly Behavior of Copolymers in a Selective Polymer Host. *Soft Matter* **2018**, *14*, 9562–9570.
- (34) Diederichsen, K. M.; McShane, E. J.; McCloskey, B. D. Promising Routes to a High Li⁺ Transference Number Electrolyte for Lithium Ion Batteries. *ACS Energy Letters* **2017**, *2*, 2563–2575.
- (35) Doyle, M.; Fuller, T. F.; Newman, J. The Importance of the Lithium Ion Transference Number in Lithium Polymer Cells. *Electrochim. Acta* **1994**, *39*, 2073–2081.
- (36) Meziane, R.; Bonnet, J. P.; Courty, M.; Djellab, K.; Armand, M. Single-Ion Polymer Electrolytes Based on a Delocalized Polyanion for Lithium Batteries. *Electrochim. Acta* **2011**, *57*, 14–19.
- (37) Bouchet, R.; Maria, S.; Meziane, R.; Aboulaich, A.; Lienafa, L.; Bonnet, J. P.; Phan, T. N. T.; Bertin, D.; Gigmes, D.; Devaux, D.; Denoyel, R.; Armand, M. Single-Ion BAB Triblock Copolymers as Highly Efficient Electrolytes for Lithium-Metal Batteries. *Nat. Mater.* **2013**, *12*, 452–457.
- (38) Inceoglu, S.; Rojas, A. A.; Devaux, D.; Chen, X. C.; Stone, G. M.; Balsara, N. P. Morphology-Conductivity Relationship of Single-Ion-Conducting Block Copolymer Electrolytes for Lithium Batteries. *ACS Macro Lett.* **2014**, *3*, 510–514.
- (39) Rojas, A. A.; Inceoglu, S.; Mackay, N. G.; Thelen, J. L.; Devaux, D.; Stone, G. M.; Balsara, N. P. Effect of Lithium-Ion Concentration on Morphology and Ion Transport in Single-Ion-Conducting Block Copolymer Electrolytes. *Macromolecules* **2015**, *48*, 6589–6595.
- (40) Villaluenga, I.; Inceoglu, S.; Jiang, X.; Chen, X. C.; Chintapalli, M.; Wang, D. R.; Devaux, D.; Balsara, N. P. Nanostructured Single-Ion-Conducting Hybrid Electrolytes Based on Salty Nanoparticles and Block Copolymers. *Macromolecules* **2017**, *50*, 1998–2005.